Operating characteristics of transcritical CO_2 heat pump for simultaneous water cooling and heating

JAHAR SARKAR[a*]
SOUVIK BHATTACHARYYA[b]

[a] Department of Mechanical Engineering Indian Institute of Technology (BHU), Varanasi, India 221005

[b] Department of Mechanical Engineering Indian Institute of Technology, Kharagpur India 721302

Abstract   The effects of water-side operating conditions (mass flow rates and inlet temperatures) of both evaporator and gas cooler on the experimental as well as simulated performances (cooling and heating capacities, system coefficient of performance (COP) and water outlet temperatures) of the transcritical CO_2 heat pump for simultaneous water cooling and heating the are studied and revised. Study shows that both the water mass flow rate and inlet temperature have significant effect on the system performances. Test results show that the effect of evaporator water mass flow rate on the system performances and water outlet temperatures is more pronounced (COP increases by 0.6 for 1 kg/min) compared to that of gas cooler water mass flow rate (COP increases by 0.4 for 1 kg/min) and the effect of gas cooler water inlet temperature is more significant (COP decreases by 0.48 for given range) compared to that of evaporator water inlet temperature (COP increases by 0.43 for given range). Comparisons of experimental values with simulated results show the maximum deviation of 5% for cooling capacity, 10% for heating capacity and 16% for system COP.

Keywords: CO_2 heat pump; Water cooling and heating; Experiment; Simulation; Performance characteristics

---

*Corresponding Author. E-mail address: js_iitkgp@yahoo.co.in

Nomenclature

c_p	–	specific heat capacity, kJ/kgK
h	–	specific enthalpy, kJ/kg
$\dot{m}$	–	mass flow rate, kg/min
N	–	compressor speed, rpm
P	–	pressure, bar
$\dot{Q}$	–	heat rate, kW
t, T	–	temperature, °C, K
UA	–	heat conductance, W/K
V_s	–	suction volume, m^3

Greek symbols

η	–	efficiency
ρ	–	density, kg/m^3

Subscripts

dis	–	discharge
ev	–	evaporator
gc	–	gas cooler
i	–	inlet
o	–	outlet
r	–	refrigerant
suc	–	suction
w	–	water
1,2,3,4	–	state points

1   Introduction

Due to twin menace of ozone layer depletion and global warming, the natural fluid CO_2 has been shown to be a promising alternative refrigerant in vapor compression refrigeration systems lately. Due to gliding temperature heat rejection in the gas cooler and design related various advantages, huge numbers of theoretical and experimental investigations have been performed within last two decades on transcrtical CO_2 cycle particularly in heat pump applications [1–3]. Neksa *et al.* [4] first experimentally investigated the effects of operating parameters on the heat pump water heater performances. After that work, most of the works published on CO_2 heat pumps within 2000s are mainly for heating applications [3]. However, works on CO_2 heat pumps for simultaneous cooling and heating are limited. Yarral *et al.* [5] experimentally investigated the effect of discharge pressure on CO_2 heat pump performance for simultaneous production of refrigeration and water heating to 90 °C for the food processing industry. White *et al.* [6] studied CO_2 heat

pump prototype for simultaneous water heating to temperature more than 65 °C and refrigeration at less than 2 °C. Adriansyah [7] experimentally studied the effect of discharge pressure for simultaneous air-conditioning and water heating. Kim *et al.* [8] have done experimental study on CO_2 heat pump to study the effect of internal heat exchanger using water as secondary fluid for both sides with emphasis only on heating. Sarkar *et al.* [9] numerically studied the effects of water inlet temperature, compressor speed and heat exchanger inventory for simultaneous water cooling and heating applications. Agrawal and Bhattacharyya [10] numerically optimized CO_2 heat pumps with capillary tube. Sarkar *et al.* [11,12] experimentally studied the performances of CO_2 heat pump for simultaneous water cooling and heating. Bhattacharyya *et al.* [13] studied CO_2 cascade system for refrigeration and heating. Byrne *et al.* [14] studied CO_2 heat pump for space cooling and heating. Yang *et al.* [15] studied water cooling and heating. Agrawal and Bhattacharyya [16] experimentally studied CO_2 heat pumps with capillary tube.

In the present investigation, both simulation and experimental results on the working prototype of a transcritical CO_2 heat pump system for simultaneous water cooling and heating are presented. The cooling and heating capacities, system COP and water outlets temperatures have been studied for various water mass flow rates and water inlet temperatures of both evaporator and gas cooler. Comparison of simulated and experimental results with other investigations is presented as well.

2 Experiments of a transcritical CO_2 heat pump

2.1 Description of test setup

Test facility layout of transcritical CO_2 heat pump for simultaneous water cooling and heating with instrumental positions is shown in Fig. 1. Stainless steel was chosen as the material for all system components. A Dorin CO_2 compressor (model TCS113: displacement = 2.2 m^3/h, capacity = 2.5 kW and rotational speed = 2900 rpm) was chosen for the experimental investigation. On the basis of minimum and maximum pressure ratios of 80/50 and 120/26 bar/bar, respectively, a Swagelok integral bonnet needle valve (model SS-1RS4) was used as the expansion device, which can be used regulate flow rate and discharge pressure/degree of superheat. The separator and receiver were designed for a total volumetric capacity of 8 and 2 l, respectively. A cooling unit including a fan and a storage tank was employed
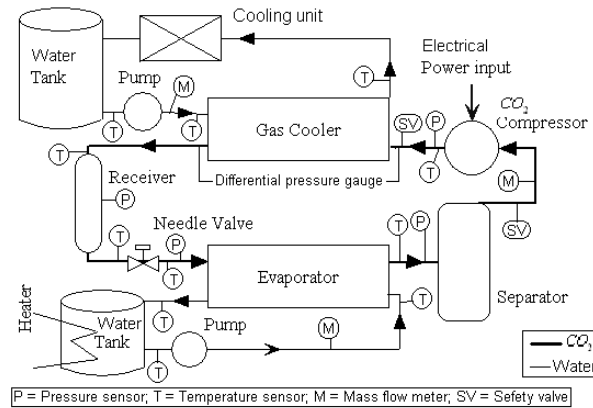
Figure 1. Test facility layout of the transcritical CO_2 heat pump.

for a maximum heat transfer rate of 6 kW to cool the warm water to its initial temperature at the inlet to the gas cooler [11]. A water bath with heater and pump was incorporated in the evaporator to supply water at constant temperature and flow rate. The evaporator and the gas cooler are counterflow tube-in-tube heat exchangers, where CO_2 flows in the inner tube and water in the outer annulus (Tab. 1). Measuring ranges of instruments with uncertainties are listed in Tab. 2 [11].

Table 1. Dimensions of gas cooler and evaporator.

Heat exchangers	Gas cooler	Evaporator
Configuration	Coaxial, Single pass, 14 rows	Coaxial, Single pass, 9 rows
Inner ID/outer OD tube diameter	6.35 mm/12 mm	9.5 mm/16mm
Total length of tubing	14 m	7.2 m

2.2   Test procedure and test conditions

In the experimental study, the effects of water inlet temperature and mass flow rate in gas cooler, and water inlet temperature and mass flow rate in evaporator were investigated by varying them using cooling unit for the gas cooler and heating unit for the evaporator. Constant suction pressure and discharge pressure were maintained by simultaneous control of the total mass of CO_2 in the system and degree of opening of the expansion device.

Table 2. Ranges and uncertainties of measuring instruments.

Parameters	Measuring instruments	Ranges	Accuracy
Pressure	Dial pressure gauge	0–160 bar	±1.5% of full range
Pressure loss	Differential pressure gauge	0–4 bar	±1.5% of full range
CO$_2$ mass flow rate	Mass flow meter	0.2–10 kg/min	±0.1% of full range
Water mass flow rate	Mass flow meter	0.5–20 kg/min	±0.5% of full range
Temperature	Thermocouples (T-type, K-type)	Calibrated range: 0–150 °C	±0.5

The total refrigerant mass in the system was controlled by adding CO$_2$ from a high pressure cylinder or by venting it through the safety valve. For certain test conditions, constant water flow rates for both evaporator and gas cooler were maintained by pumps, water inlet water temperature to gas cooler was maintained by controlling fan speed and water inlet temperature to evaporator was maintained by heater control. The compressor power input was measured by using a power meter, the refrigerant mass flow rate was measured by a Coriolis effect flow meter, the pressure of the refrigerant were monitored by using pressure transducers, pressure drop in the heat exchangers was measured by differential pressure transducer and refrigerant and water temperatures at all required locations were measured by using T-type and K-type thermocouples. All the measurements have been done at steady state condition. The principal system performance parameters under steady state, namely, power input to the compressor, cooling capacity, heating capacity, system coefficient of performance (COP) have been computed from the measured data. The uncertainties of cooling capacity, heating capacity and system COP, estimated by error analysis, are approximately ±5%, ±5% and ±6%, respectively [12].

3   Simulation of transcritical CO$_2$ heat pump

The simulated CO$_2$ based heating and cooling system consists of compressor, expansion valve, evaporator and gas cooler. Water is taken as secondary fluid for both gas cooler and evaporator to give the useful cooling and heating outputs. Both these heat exchangers are of double-pipe

counter flow type, where the refrigerant flows through the inner tube and water flows through the outer annular space. The layout and corresponding temperature-entropy diagram with water flow lines is shown in Fig. 2.
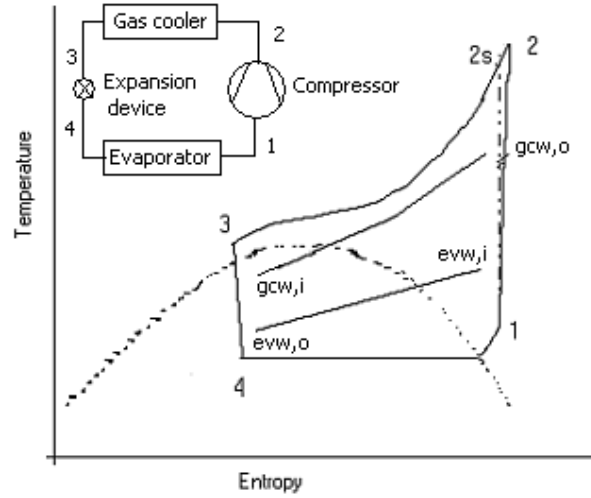

Figure 2. Cycle process temperature-entropy diagram of a transcritical CO_2 heat pump.

The entire system has been modeled based on energy balance of individual components yielding conservation equations presented below. The following assumptions have been made in the analysis:

1. Heat transfer with the ambient is negligible.

2. Only single-phase heat transfer occurs for water (external fluid).

3. Compression process is adiabatic but not isentropic.

4. Pressure drop on waterside and in connecting pipes are negligible.

5. Changes in kinetic and potential energies are negligible.

6. Refrigerant is free from oil.

3.1   Compressor model

The refrigerant mass flow rate through the compressor is given by [11]

$$\dot{m}_r = \rho_1 \eta_v V_s \frac{N}{60} \, , \tag{1}$$

where η_v is the volumetric efficiency. The following correlations have been used for volumetric and isentropic efficiencies respectively for the semi-hermetic compressor $(\eta_{is,c})$, which have obtained based on regression of manufacturer test data, neglecting the effect of degree of superheat [11]:

$$\eta_v = 1.1636 - 0.2188 \left(\frac{P_{dis}}{P_{suc}} \right) + 0.0163 \left(\frac{P_{dis}}{P_{suc}} \right)^2 , \qquad (2)$$

$$\eta_{is,c} = 0.61 + 0.0356 \left(\frac{P_{dis}}{P_{suc}} \right) - 0.0257 \left(\frac{P_{dis}}{P_{suc}} \right)^2 + 0.0022 \left(\frac{P_{dis}}{P_{suc}} \right)^3 . \quad (3)$$

3.2 Gas cooler model

To consider the lengthwise property variation, gas cooler has been discretized into equal length segments along the refrigerant flow direction and momentum and energy conservation equations have been applied to each segment [9–10]. Employing log mean temperature difference (LMTD) expression, heat transfer in i-th segment of the gas cooler (gc) is given by,

$$Q_{gc}^i = (UA)_{gc}^i \frac{(T_{gcr}^i - T_{gcw}^i) - (T_{gcr}^{i+1} - T_{gcw}^{i+1})}{\ln \left(\frac{T_{gcr}^i - T_{gcw}^i}{T_{gcr}^{i+1} - T_{gcw}^{i+1}} \right)} . \qquad (4)$$

Additionally, energy balance in segment of gas cooler for both the fluids yield

$$Q_{gc}^i = \dot{m}_r (h_{gcr}^i - h_{gcr}^{i+1}) = \dot{m}_{gcw} c_{pw} (T_{gcw}^i - T_{gcw}^{i+1}) . \qquad (5)$$

The overall heat transfer coefficient for the segment of gas cooler has been calculated using the fundamental equation for overall heat transfer coefficient.

To estimate the heat transfer coefficient of supercritical carbon dioxide for in-tube cooling in gas cooler, Pitla *et al.* [17] correlation, incorporating both bulk and wall properties due to large variation of fluid properties in the radial direction, has been used. The pressure drop for supercritical carbon dioxide in-tube cooling has been calculated by Petrov and Popov equation [18], neglecting inertia effect. The waterside heat transfer coefficient has been evaluated by the Gnielinski [17] equation for annular flow. All water properties are assumed to be temperature dependent only, and polynomial expressions based on text book values have been used.

3.3   Evaporator model

The evaporator consists of two zones: two-phase (boiling) zone and super-heated zone. Similar to the gas cooler, both zones in the evaporator are divided into a finite number of equal-length segments along the refrigerant flow direction. Each segment is treated as one counter-flow heat exchanger and the outlet conditions of each segment should become inlet conditions for the next segment. For each segment LMTD method is used and properties are evaluated based on mean temperature and pressure. Energy balance in each segment of the evaporator (ev) for the refrigerant (CO_2) and water, respectively, yields

$$Q_{ev}^i = \dot{m}_r(h_{evr}^{i+1} - h_{evr}^i) = \dot{m}_{evw}c_{pw}(T_{evw}^{i+1} - T_{evw}^i) \,. \tag{6}$$

The overall heat transfer coefficient for each segment of the evaporator has been calculated in the same way as for the gas cooler. In this analysis, the recently developed Yoon *et al.* [19] correlation has been employed to estimate the boiling heat transfer coefficient. For superheated zone, Gnielinski [17] equation has been used to estimate convective heat transfer coefficient of carbon dioxide. Jung and Radermacher [20] correlation has been used for boiling pressure drop and Blasius correlation has been used for single phase pressure drop of carbon dioxide. The waterside heat transfer coefficient has been evaluated by Gnielinski [17] equation for annular flow for both two-phase and superheated sections.

Using discretization, the heat exchanger is made equivalent to a number of counter flow heat exchangers arranged in series and the combined heat transfer of all the segments is the total heat transfer of the heat exchanger. Therefore, fast changing properties of CO_2 have been modeled accurately in both evaporator and gas cooler.

3.4   Expansion device model

Dissimilar to the subcritical cycle, the needle valve is used to mainly control the high-side pressure, not superheating in the experiment. Small super-heating was experienced, although the superheating may be neglected due to use of separator. For simplicity, the expansion process is considered to be isenthalpic under the assumption that the heat exchange with its surroundings is negligible, yielding [11]

$$h_4 = h_3 \,. \tag{7}$$

3.5 Numerical procedure

A computer code, incorporating the subroutine CO2PROP [9] for thermo-physical and transport properties, has been developed to simulate the transcritical carbon dioxide system for simultaneous water cooling and heating at various operating conditions. Water inlet temperatures and water mass flow rates for both heat exchangers, compressor data, evaporator and gas cooler dimensions, compressor suction pressure and discharge pressure are the input data for the simulation.
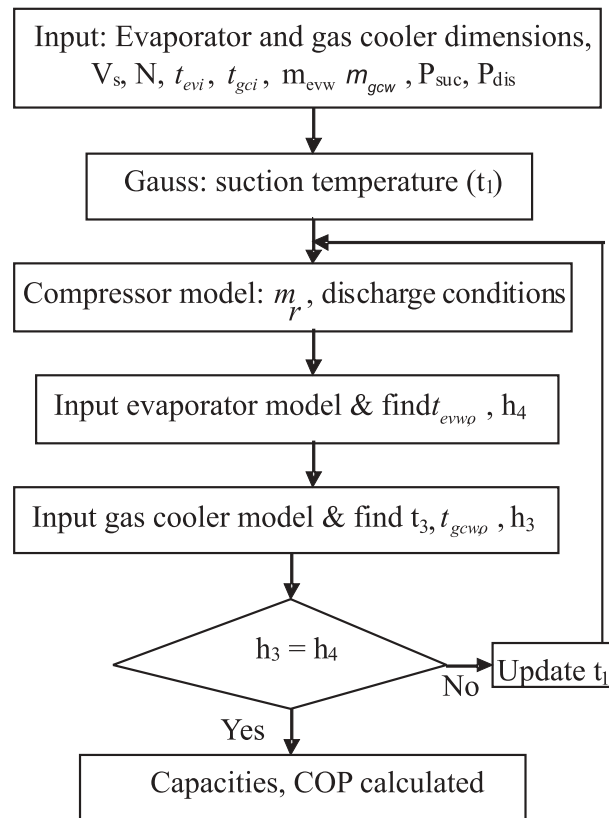

Figure 3. Flow-chart for the simulation model.

The flow chart of the simulation is shown in Fig. 3. Pressure drop and heat loss in connecting lines are not considered, therefore, the outlet state of one component becomes the inlet state of the next component. In the simulation, by assuming the suction temperature, refrigerant mass flow rate

and compressor outlet conditions are calculated by compressor model, and
refrigerant conditions at evaporator inlet and at gas cooler outlet as well as
water outlet temperatures of both evaporator and gas cooler are calculated
based on mathematical model of evaporator and gas cooler. The suction
temperature is adjusted by the iteration in order for the enthalpy of inlet
(h_3) and outlet (h_4) of expansion valves to converge within a prescribed tol-
erance and performances such as cooling and heating capacities, compressor
work and COP are calculated. Tolerance has been maintained in the range
of 10^{-3} for simulation.

4   Results and discussion

The performance of the CO_2 heat pump system in terms of cooling and
heating capacities and system COP (cooling + heating capacities divided
by compressor power) considering both cooling and heating as useful out-
puts are studied for the suction and discharge pressure of 40 and 90 bar,
respectively. It may be noted that the different mass flow rate ranges have
been taken for gas cooler and evaporator due to the limitation of water pump
capacities in experimental setup. Both the numerical and experimental re-
sults are presented to study the effect of water inlet temperatures (25 to
35 °C for evaporator and 30 to 40 °C for gas cooler) and mass flow rates
(1 to 3 kg/min for evaporator and 0.7 to 2 kg/min for gas cooler) on the
performances and water outlet temperatures. Unless otherwise specified,
constant values of operating parameters are: evaporator water inlet tem-
perature of 29 °C, gas cooler water inlet temperature of 33 °C, evaporator
water flow rate of 1.5 kg/min and gas cooler water flow rate of 1 kg/min.

Effects of water mass flow rate to evaporator on the system perfor-
mances and water outlet temperatures for both gas cooler and evaporator
are shown in Figs. 4 and 5, respectively. With increase in water mass flow
rate to evaporator, the cooling capacity increases due to increase in water
side heat transfer coefficient and both the heating capacity and compressor
work increase modestly due to minor increase in the suction temperature
(increase in degree of superheat) and also discharge temperature. Water
outlet temperature of evaporator increases due to dual effect of increase in
cooling capacity and water mass flow rate; whereas water outlet tempera-
ture of gas cooler increases due to increase in heating capacity. Similar to
earlier study [6], both heating capacity and COP increase with decrease in
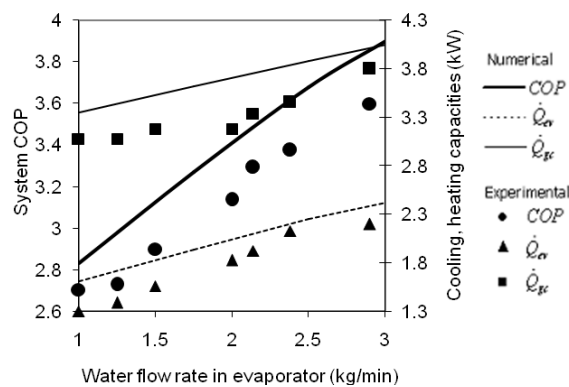hot water outlet temperature.

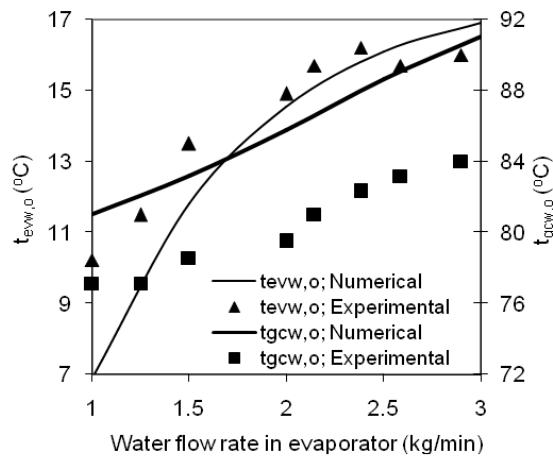Figure 4. System performance variation with evaporator water flow rate.

Figure 5. Water outlet temperature variation with evaporator water flow rate.

Effects of water mass flow rate to gas cooler on the performances and water outlet temperatures for both gas cooler and evaporator are shown in Figs. 6 and 7, respectively. With increase in water mass flow rate in gas cooler, heating output increases modestly due to increase in water side heat transfer coefficient and refrigerant mass flow rate increases, which enhances the cooling capacity, although the effect on compressor work is insignificant and hence the system COP increases. Due the dual effect of increase in water mass flow rate and heating capacity, the water outlet temperature of
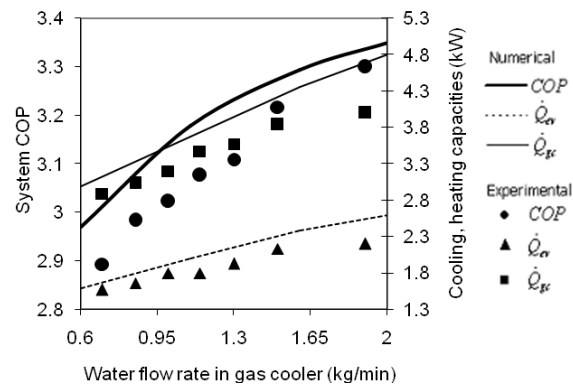
Figure 6. Variation of system performance with gas cooler water flow rate.
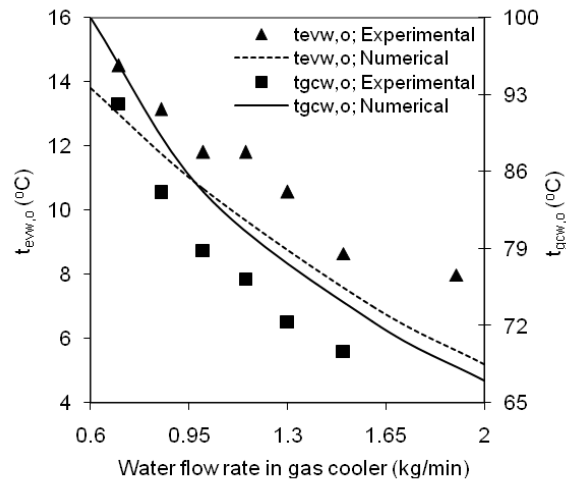

Figure 7. Variation of water outlet temperatures with gas cooler water flow rate.

gas cooler decreases and evaporator water outlet temperature decreases due to increase in cooling capacity with increase in water mass flow rate in gas cooler. Results show that the effect of water flow rate in evaporator is more pronounced on the performances (COP increases about 0.6 per 1 kg/min) compared to the effect of water mass flow rate in gas cooler (COP increases about 0.4 per 1 kg/min).

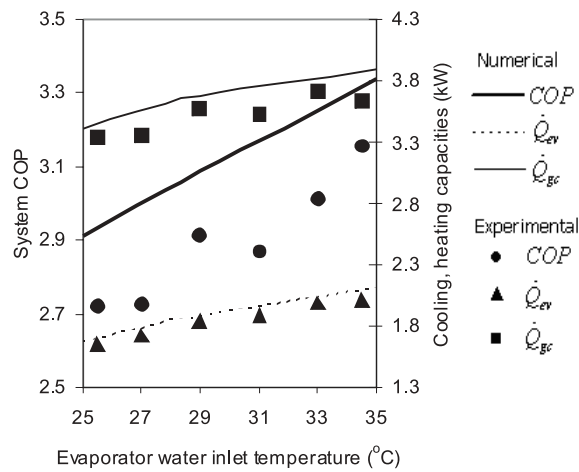Figures 8 and 9 exhibit the variations of performances and water out-

Figure 8. Variation of system performance with evaporator water inlet temperature.
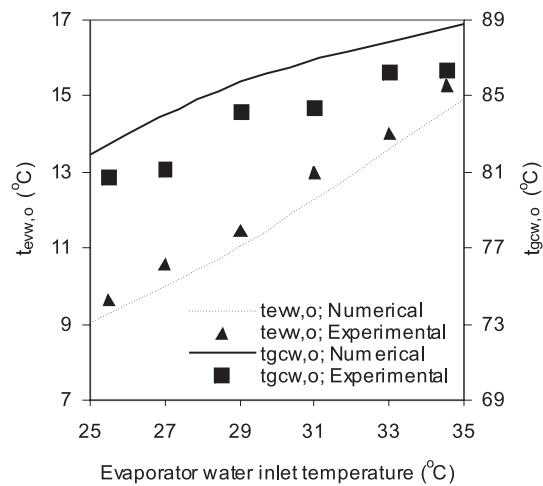

Figure 9. Water outlet temperature variation with evaporator water inlet temperature.

let temperatures with the evaporator water inlet temperature. With the increase in water inlet temperature to evaporator, suction temperature as well as discharge temperature increases, which enhance both cooling and heating capacities; however compressor work increases insignificantly due to nearly constant refrigerant mass flow rate and hence system COP increases.

Similar trends have been observed for the cycles with capillary tube expansion [16] and work recovery device expansion [15] also. It may be noted that the mass flow rate of refrigerant is nearly invariant with the water mass flow rates and water inlet temperatures due to conditions applied (constant suction and discharge pressures, dissimilar to the earlier study [9]) in the present case. The performances change mainly due to change in water side heat transfer characteristics. Water outlet temperature of evaporator increases due to dual effect of increase in cooling capacity and water inlet temperature; whereas water outlet temperature of gas cooler increases due to increas e in heating capacity.
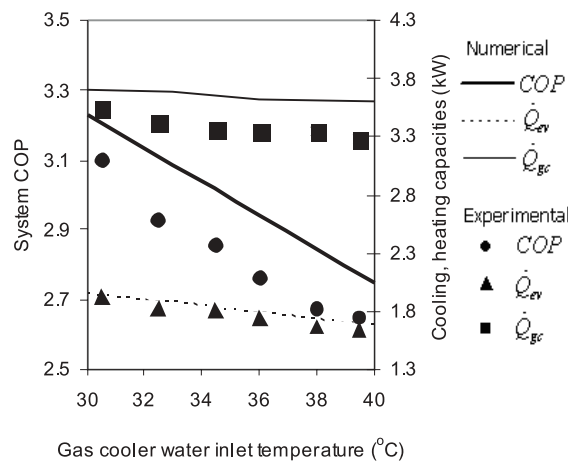

Figure 10. Variation of system performance with gas cooler water inlet temperature.

Figures 10 and 11 exhibit the variations of performances and water outlet temperatures with water inlet temperature to gas cooler. As the water inlet temperature to gas cooler increases, the heating capacity decreases due to deterioration in heat transfer properties of CO_2 in gas cooler and the refrigerant exit temperature in gas cooler increases, which increases the vapor quality in evaporator inlet and hence cooling output also decreases, however, compressor work is nearly invariant due to negligible change in refrigerant mass flow rate and degree of superheat and hence system COP decreases significantly similar to the earlier studies [8–12]. Similar trend has been observed with internal heat exchanger also [21]. Due the dual effect of increase in water inlet temperature and decrease in heating capacity, the water outlet temperature of gas cooler increases and evaporator water outlet
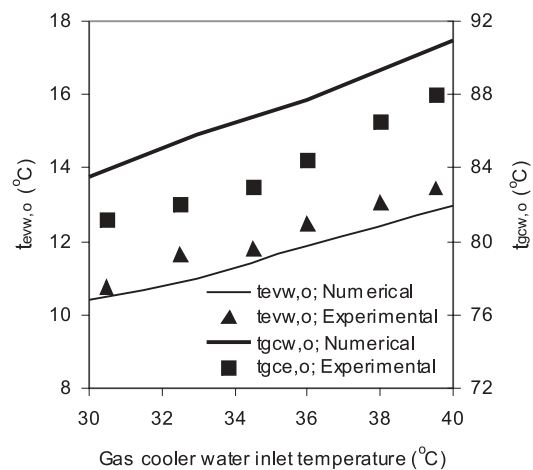
Figure 11. Water outlet temperature variation with gas cooler water inlet temperature.

temperature increases due to decrease in cooling capacity with increase in water inlet temperature to gas cooler. Results show that the effect of water inlet temperature to gas cooler on the system performances is more significant (COP decreases by about 0.48 per 10 °C) compared to the effect of water inlet temperature to evaporator (COP increases about 0.43 per 10 °C water inlet temperature).

As stated above, due to limitation of pump capacities, results have not been shown for higher mass flow rates in gas cooler and evaporator. However, the numerical results show that the performance improves although improvement rate decreases gradually with increase in mass flow rates in both gas cooler and evaporator. Results show that the test values of heating capacity is lower than the simulated values with maximum deviation of 5%, test values of heating capacity are lower than the simulated values with maximum deviation of 10% and experimental values of COP is lower than the simulated values with maximum deviation of 16%. Results show that the test values of water outlet temperature to evaporator are higher than the simulated values with maximum deviation of 12% and that is lower in case of gas cooler with maximum deviation of 7.5%. It may be noted that the suction pressure is maintained constant by varying degree of superheat unlike to the previous studies [9–10] and the superheat values varied from 5 to 15 °C in the simulation and to 20 °C in the test for given ranges.

5 Conclusions

Both simulation and experimental studies on a transcritical CO_2 heat pump system for simultaneous water cooling and heating have been carried out to study the system performances and water outlet temperatures for various mass flow rates and water inlet temperatures for both evaporator and gas cooler. The cooling and heating capacities and COP increase with increase in water mass flow rate to both evaporator and gas cooler, however, effect is more pronounced in case of evaporator mass flow rate (COP increases by 0.6 per 1 kg/min, whereas 0.4 for gas cooler mass flow rate). Evaporator and gas cooler water outlet temperatures increase with increase in evaporator mass flow rate and decrease with increase in evaporator mass flow rate. Cooling and heating capacities as well as COP increase with increase in water inlet temperature to evaporator, whereas trends are opposite with increase in gas cooler water inlet temperature; effect of gas cooler water inlet temperature is more pronounced (COP increases by 0.48 per 10 °C, whereas 0.43 for gas cooler). With the increase in water inlet temperatures to both evaporator and gas cooler, water outlet temperatures of both evaporator and gas cooler increase. Comparison of simulated and experimental values showed the maximum deviation of 5% for cooling capacity, 10% for heating capacity, 16% for system COP, 12% and 7.5% for water outlet temperatures of evaporator and gas cooler, respectively.

Received 23 March 2012

References

[1] NEKSA P.: *CO₂ heat pump systems.* Int. J. Refrigeration **25**(2002), 421–427.

[2] KIM M.H., PETTERSEN J., BULLARD C.W.: *Fundamental process and system design issues in CO₂ vapor compression systems.* Prog. Energ. Combust. Sci. **30**(2004), 119–174.

[3] AUSTIN B.T., SUMATHY K.: *Transcritical carbon dioxide heat pump systems: A review.* Renew. Sust. Energ. Rev. **15**(2011), 4013–4029.

[4] NEKSA P., REKSTAD H., ZAKERI G.R., SCHIEFLOE P.A.: *CO₂ heat pump water heater: characteristics, system design & experimental results.* Int. J. Refrig. **21**(1998), 172–179.

[5] YARRAL M.G., WHITE S.D., CLELAND D.J., KALLU R.D.S., HEDLEY R.A.: *Performance of transcritical CO$_2$ heat pump for simultaneous refrigeration and water heating.* In: XX Int. Congress of Refrigeration, Sydney, 1999, Paper 651.

[6] WHITE S.D., YARRALL M.G., CLELAND D.J., HEDLEY R.A.: *Modelling the performance of a transcritical CO$_2$ heat pump for high temperature heating.* Int. J. Refrig. **25**(2002), 479–486.

[7] ADRIANSYAH W.: *Combined air conditioning and tap water heating plant using CO$_2$ as refrigerant.* Energy Buildings **36**(2004), 690–695.

[8] KIM S.G., KIM Y.J., LEE G., KIM M.S.: *The performance of a transcritical CO$_2$ cycle with an internal heat exchanger for hot water heating.* Int. J. Refrig. **28**(2005), 1064–1072.

[9] SARKAR J., BHATTACHARYYA S., RAMGOPAL M.: *Simulation of a transcritical CO$_2$ heat pump cycle for simultaneous cooling and heating applications.* Int. J. Refrig. **29**(2006), 735–743.

[10] AGRAWAL N., BHATTACHARYYA S.: *Optimized transcritical CO$_2$ heat pumps: Performance comparison of capillary tubes against expansion valves.* Int. J. Refrig., **31**(2008), 388–395.

[11] SARKAR J., BHATTACHARYYA S., RAMGOPAL M.: *A transcritical CO$_2$ heat pump for simultaneous water cooling and heating: Test results and model validation.* Int. J. Energy Res. **33**(2009), 100–109.

[12] SARKAR J, BHATTACHARYYA S, RAMGOPAL M.: *Experimental investigation of transcritical CO$_2$ heat pump for simultaneous water cooling and heating.* Therm. Sci. **14**(2010), 57–64.

[13] BHATTACHARYYA S., GARAI A., SARKAR J.: *Thermodynamic analysis and optimization of a novel N$_2$O-CO$_2$ cascade system for refrigeration and heating.* Int. J. Refrig. **32**(2009), 1077–1084.

[14] BYRNE P., MIRIEL J., LENAT Y.: *Design and simulation of a heat pump for simultaneous heating and cooling using HFC or CO$_2$ as a working fluid.* Int. J. Refrig.**32**(2009), 1711–1723.

[15] YANG J.L., MA Y.T., LI M.X., HUA J.: *Modeling and simulating the transcritical CO$_2$ heat pump system.* Energy Int. J. **35**(2010), 4812–4818.

[16] AGRAWAL N., BHATTACHARYYA S.: *Experimental investigations on adiabatic capillary tube in a transcritical CO$_2$ heat pump system for simultaneous water cooling and heating.* Int. J. of Refrig. **34**(2011), 476–483.

[17] PITLA S.S., GROLL E.A., RAMADHYANI S.: *New correlation to predict the heat transfer coefficient during in-tube cooling of turbulent supercritical CO$_2$.* Int. J. Refrig. **25**(2002), 887–895.

[18] FANG X., BULLARD C.W., HRNJAK P.S.: *Heat transfer and pressure drop of gas coolers.* ASHRAE Trans. **107**(2001), 255–266.

[19] YOON S.H., CHO E.S., HWANG Y.W., KIM M.S., MIN K., KIM Y.: *Characteristics of evaporative heat transfer and pressure drop of carbon dioxide and correlation development.* Int. J. Refrig. **27**(2004), 111–119.

[20] Jung D.S., Radermacher R.: *Prediction of pressure drop during horizontal annular flow boiling of pure and mixed refrigerants.* Int. J. Heat Mass Tran. **32**(1989), 2435–2466.

[21] Goodman C., Fronk B.M., Garimella S.: *Transcritical carbon dioxide microchannel heat pump water heaters: Part II – System simulation and optimization.* Int. J. Refrig. **34**(2011), 870–880.